

Dependence of multiple Mn^{2+} spin-flip Raman scattering in quantum wells on the magnetic field direction

L. C. Smith, J. J. Davies, and D. Wolverson

Department of Physics, University of Bath, Bath BA2 7AY, United Kingdom

M. Lentze and J. Geurts

Physikalisches Institut, Experimentelle Physik III, Universität Würzburg, Am Hubland, 97074 Würzburg, Germany

T. Wojtowicz and G. Karczewski

Institute of Physics, Polish Academy of Sciences, 02668 Warsaw, Poland

(Received 14 November 2007; revised manuscript received 18 February 2008; published 20 March 2008)

We show that the number n_{max} of simultaneous manganese paramagnetic resonance spin flips observed in the Raman spectra of a CdMnTe/CdMnMgTe quantum well monotonically decreases as the angle between the external magnetic field and the quantum well growth axis is varied from 90° to 0° . The appearance of the multiple spin flips is due to precession of the manganese spins about the resultant field formed by combining the external magnetic field with the exchange field due to heavy-holes in the intermediate state of the scattering process. In our experiments, the exchange field is well defined and this has enabled us to provide a test of a model previously proposed for the process. We find good agreement between the experiment and the theoretical predictions.

DOI: 10.1103/PhysRevB.77.115341

PACS number(s): 73.61.Ga, 73.63.Hs, 75.50.Pp, 78.30.-j

I. INTRODUCTION

The observation of multiple paramagnetic resonance (PMR) spin-flip Raman scattering lines due to Mn^{2+} ions in CdMnTe-based quantum wells when a magnetic field \mathbf{B}_{ext} is applied perpendicular to the light propagation direction and quantum well growth direction (z) has been well documented.¹⁻³ In this Raman scattering process, the shift in energy between incident and emitted photons is equal to an integer multiple n of the basic PMR energy, $\Delta E = g_{Mn} \mu_B B_{eff}$, where μ_B is the Bohr magneton and where the gyromagnetic ratio for the Mn^{2+} $3d^5$ electrons is $g_{Mn} \sim 2$. Frequently, PMR signals with large values of n are observed (up to $n=19$); this cannot be explained in terms of scattering processes involving the six $[(2S+1)]$, with $S=5/2$ spin states of a single Mn^{2+} ion¹ and, instead, the phenomenon must be a collective effect involving several Mn^{2+} ions.

One model for the process is as follows.¹ The intermediate state in the Raman scattering process consists of a localized heavy-hole exciton. In the presence of an external magnetic field \mathbf{B}_z along the growth direction (the z axis), the heavy-hole states are characterized by $J_z = \pm 3/2$, being split apart in energy by an amount we can write as $3g_{||}^h \mu_B B_z$, where $g_{||}^h$ defines the effective hole g value (in a magnetic semiconductor, $g_{||}^h$ is considerably enhanced by the exchange interaction with the magnetic ions and, given our definition, is itself field dependent).

When the external magnetic field \mathbf{B}_{ext} is at an angle θ to the z axis, the states $J_z = \pm 3/2$ remain unmixed, provided that these heavy-hole states are well separated in energy from those of the light-holes (for example, as is the case under very strong quantum confinement). In this approximation, J_z remains a good quantum number and the manganese ions in the vicinity of the exciton experience a strong exchange field \mathbf{B}_{exch} directed along the z direction, in addition

to the externally applied field. In the intermediate state, the total magnetization of these manganese ions thus begins to precess about the total field $\mathbf{B}_{eff} = \mathbf{B}_{ext} + \mathbf{B}_{exch}$ with angular velocity $\omega_L = g_{Mn} \mu_B B_{eff} / \hbar$, as shown in Fig. 1. At time t later, recombination occurs; at this time, the magnetization has precessed through an angle $\omega_L t$ and its projection in the direction of the external field has decreased, so that the system returns to a new ground state in which the magnetization is less than its original value. This decrease in magnetization corresponds to the multiple spin flips that are observed in the Stokes spin-flip Raman (SFR) spectrum. The model also predicts that multiple spin flips will not be observed in the anti-Stokes spectrum, in agreement with experiment. This model was introduced in Ref. 1 to account for multiple Mn^{2+} SFR signals observed with the field in the plane of the quantum well and was also applied to the interpretation of femtosecond time-resolved measurements of the induced Faraday rotation^{4,5} and in a discussion of optically induced quantum entanglement² in similar systems. However, a difficulty with this simple viewpoint was highlighted in Ref. 6.

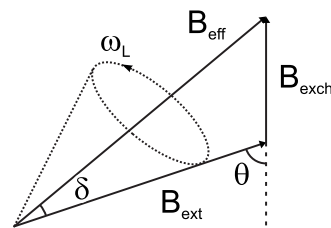


FIG. 1. Vector diagram of the externally applied and exchange fields (\mathbf{B}_{ext} and \mathbf{B}_{exch} , respectively) and the effective magnetic field \mathbf{B}_{eff} that is produced for an arbitrary orientation of the external field to the quantum well growth axis (the latter lies in the direction of the dashed line). Adapted from Ref. 1.

The problem is as follows. If, as assumed above, the light-hole states are energetically well removed from the heavy-hole states, the heavy-hole spin states $J_z = \pm 3/2$ become degenerate when the external field is in the plane of the quantum well (the effective heavy-hole g value g_{\perp}^h becomes zero); J_z nevertheless remains a good quantum number. However, if the light-hole states lie close in energy to the heavy-holes, they can be mixed with the heavy-hole states as a result of the interaction with the external magnetic field. This mixing can be significant since the effective g values for the holes are very large (due to the enhancement of the external magnetic field by the exchange interaction with the magnetic ions). As a result, J_z is no longer a good quantum number [the heavy-hole states now involve the combinations $(|+3/2\rangle \pm |-3/2\rangle)/\sqrt{2}$ and g_{\perp}^h becomes finite]. There is therefore no net exchange field \mathbf{B}_{exch} in the intermediate state, and multiple Mn^{2+} SFR transitions would not at first sight be expected. To account for this apparent conflict between theory and experiment, the theory was extended in Ref. 6, where it was shown that, even in the presence of a finite in-plane g factor g_{\perp}^h , multiple spin-flip scattering can occur.

The investigations to date have involved magnetic fields orientated either along the z direction ($\theta=0^\circ$) or perpendicular to it ($\theta=90^\circ$). The purpose of the present paper is to report experiments for which the magnetic field is at intermediate angles, as illustrated in Fig. 1. Under these circumstances, the heavy-hole spin component in the z direction in the intermediate state remains well defined and the data present a direct test of the multiple spin-flip model in its original simple form. At low temperature, the magnetization of the manganese ions in the initial state is given by $-g_{\text{Mn}}\mu_B I$, where $I = n_{\text{Mn}}S$. For the manganese concentrations in the present specimens, the number n_{Mn} of Mn^{2+} ions within the exciton volume is of order 20 and $S=5/2$, so that $I \sim 50$. The fractional changes in magnetization (corresponding to ΔI in the range of 1–10) that we shall discuss are therefore relatively small.

We also note that a recent study³ showed multiple PMR signals ($n \leq 7$) with external fields *parallel* to the quantum well normal ($\theta=0$), which the precession model outlined above cannot explain; it was suggested that such an explanation may be incomplete and that other mechanisms of Mn-Mn interaction may also play a role. However, in the present experiments, we find that no multiple ($n > 2$) Mn^{2+} PMR transitions are seen for $\theta=0$ and find that additional Mn^{2+} - Mn^{2+} interactions are not necessary to account for the behavior, which we shall see that it can be satisfactorily explained in terms of the precession model.

II. EXPERIMENTAL DETAILS

The experimental arrangement for spin-flip Raman spectroscopy is described in detail in Ref. 7. The excitation source was a Ar^+ -ion pumped Ti-sapphire laser and the excitation was resonant with the lowest-energy excitonic state of the sample. This was a 45 Å wide $\text{Cd}_{1-x}\text{Mn}_x\text{Te}/\text{Cd}_{1-x-y}\text{Mn}_x\text{Mg}_y\text{Te}$ quantum well; the well and barrier compositions were given by $x=0.0116$ and $y=0.12$.

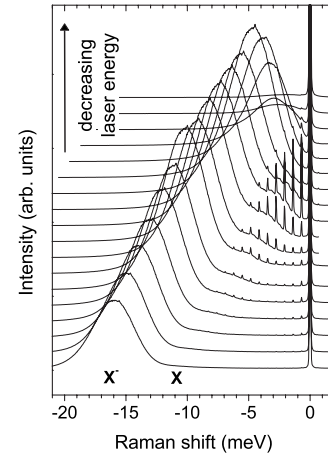


FIG. 2. Spin-flip Raman spectra for a series of excitation energies at a magnetic field of 6 T for a 45 Å wide $\text{Cd}_{1-x}\text{Mn}_x\text{Te}/\text{Cd}_{1-x-y}\text{Mn}_x\text{Mg}_y\text{Te}$ quantum well ($x=0.0116$ and $y=0.12$). The excitation energies range in 0.92 meV steps from 1.6789 eV (bottom) to 1.6633 eV (top), and the positions of the X^- and X^+ PL bands are indicated for the bottom spectrum.

The Mn^{2+} concentration x was chosen to be the same in the well and in the barrier to avoid changes in the distribution of magnetic ions at the interfaces. The sample was held inside a split-coil superconducting magnet at a nominal temperature of 1.5 K. The magnet could be orientated so that the propagation direction \mathbf{k} of the excitation beam corresponded either to the Voigt ($\mathbf{B}_{\text{ext}} \perp \mathbf{k}$) or to the Faraday ($\mathbf{B}_{\text{ext}} \parallel \mathbf{k}$) geometry. The sample could be freely turned about the axis perpendicular to both \mathbf{k} and \mathbf{B}_{ext} such that the angle θ between the growth axis and (\mathbf{B}_{ext}) could be continuously adjusted from 0° (Faraday) to 90° (Voigt).

III. RESULTS AND DISCUSSION

Figure 2 shows spectra exhibiting the multiple PMR signals at a magnetic field of 6 T in the Voigt geometry. The excitation source was tuned from 1.6633 to 1.6789 eV, close to the energy range of the photoluminescence (PL) bands arising from the free (or weakly localized) heavy-hole exciton (X , $e1-hh1$ in conventional notation) and, at lower-energy, the donor-bound (D^0X) or charged exciton (X^-). The identity of the lower energy band is not relevant to this work since, as is seen in Fig. 2, excitation in resonance with it does not lead to the observation of multiple ($n > 2$) PMR signals; however, on the grounds outlined in Ref. 8, we believe it to be X^- .

There is an enhancement of the Raman signal intensity when the energy of either the ingoing or outgoing photon is equal to that of one of the exciton states. Thus, for example, the fifth spectrum from the bottom in Fig. 2 shows PMR signals with low n ($n=1, \dots, 3$), which are in ingoing resonance, and with high n ($n \sim 9$), which are in outgoing resonance, while the signals with intermediate values of n are much weaker. At the higher end of the laser tuning range, we can observe up to the 13th PMR overtone in this way.

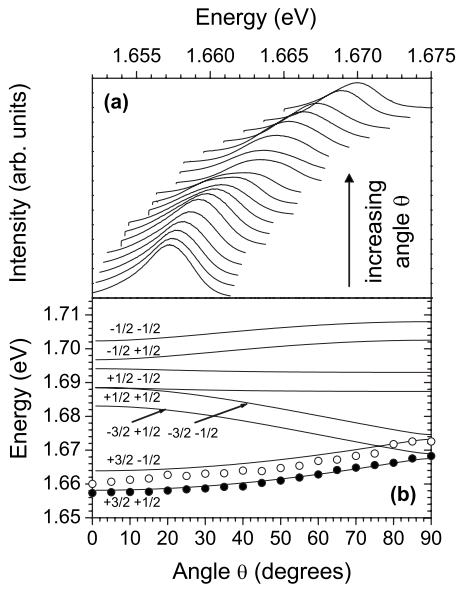


FIG. 3. (a) Dependence of the photoluminescence spectra on the angle θ between the growth axis and the external magnetic field ranging from 0° to 90° at a magnetic field of 6 T. (b) Transition energies of the free exciton X as a function of θ : PL data (solid circles) and simulated data (solid lines). Also shown is the excitation energy used at each angle to obtain the PMR Raman signals (open circles). The transitions are labeled by the basis functions $|m_j, m_s\rangle$ (quantized along the growth axis z) relevant strictly to $\theta=0^\circ$ only.

Since resonant effects clearly influence the number of detectable PMR overtones, it is essential to take them into account in studying the angle dependence of the PMR signals. The energy of the excitonic transitions and, hence, that of the optical resonance conditions is strongly dependent on θ . This is shown in the angle-dependent PL spectra [Fig. 3 (upper panel)]. As in Fig. 2, the PL spectra are made up of a strong peak (X^-) with a weak and unresolved shoulder on the high-energy side (X). The angle-dependent energy position of the latter (X) is plotted (filled circles) in Fig. 3 (lower panel). The solid lines are the eigenenergies of the Hamiltonian,

$$H = \mu_B(g_e^* \sigma \cdot B + g_h^* J \cdot B) + \Delta\sigma \cdot J + \Delta H_{ex} + D \left[J_z^2 - \frac{1}{3} J(J+1) \right]. \quad (1)$$

Here, the first and second terms are the electron and hole Zeeman components with effective g factors g_e^* and g_h^* , respectively, and the third term represents the electron-hole exchange interaction.

The single-particle confinement of electrons and holes in the quantum well leads to an increase in the excitonic band gap represented by the fourth term ΔH_{ex} as well as a splitting between light- and heavy-holes due to their confinement. Here, this splitting (energy $2D$) is represented in the simplest possible model by the last term, which is diagonal and equivalent in form to a term arising from a strain in the z direction. Although one should, in principle, solve the 4×4 Kohn-Luttinger Hamiltonian for the hole envelope wave

functions including off-diagonal terms,⁹ here, it has been previously shown that the model that we have used can give a reasonable description of the magneto-optics of quantum wells given a sufficiently large separation in energy of the light- and heavy-holes.^{10,11} Here, a test of the validity of this model is in agreement between calculated and experimental data for the PL as a function of angle [shown in Fig. 3(b)]. In this figure, we also show the higher-energy exciton states, labeled by the spin quantum numbers $|m_j, m_s\rangle$ relevant to the Faraday geometry $\theta=0^\circ$. They demonstrate for this particular quantum well that the zero-field splitting of the hole states is sufficient for the exciton states to show clear light- or heavy-hole character over the whole angle range.

The electron and hole Zeeman splittings (giving $g_{e,h}^*$) depend on the magnetic field and are described by a Brillouin-function behavior whose parameters were experimentally determined from observation of the conduction band electron spin-flip Raman scattering (this signal is, in fact, present under the conditions of Fig. 2, though it is not easily visible in that figure). Other parameters were estimated from literature values (e.g., effective masses,^{10,12} band gaps,¹³ and offsets^{8,14}) or typical magnitudes (e.g., electron-hole exchange of 0.1 meV). In the absence of a magnetic field, the calculated energies agreed well with experimental transition energies for the $e1-hh1$ and $e1-lh1$ exciton states determined via reflectivity measurements. Good agreement is then found between the simulations and the experimental data for the lowest-energy excitonic PL transition in a magnetic field, as shown in Fig. 3(b), indicating only a small Stokes' shift between emission and absorption (of order 1 meV). The calculation also provides insight into the degree of mixing of light- and heavy-holes in this particular quantum well and, in Fig. 4, we show the squared amplitudes of the joint electron-hole states (in the basis quantized along the quantum well normal, i.e., the z direction) that make up the lowest-energy exciton state over the angle range $0^\circ < \theta < 90^\circ$. Figure 4 shows that J_z remains a good quantum number over the range from $\theta=0$ to $\theta \approx 80^\circ$.

In the present experiments, the excitation energy for the PMR Raman spectra was chosen to maximize the number of detectable overtones and their strength while *at the same time* preserving a monotonic decrease in the overtone intensity where possible. In the range $75^\circ < \theta < 90^\circ$, higher-lying exciton states are converging with the resonant intermediate state selected for the experiment (see Fig. 3) and so the relative overtone intensities show a slight effect due to a second resonance condition. Under these circumstances, values of n up to 8 were observed for large values of θ (signals with larger values of n can be observed with different tuning of the laser, but the variation in intensities is no longer monotonic in n). Given these requirements, the resonant excitation energy was found to follow the same trend with angle as the PL energy, as shown in Fig. 3 (open circles), and is found to lie between the two exciton states lowest in energy which must, therefore, be the two states providing simultaneous ingoing and outgoing resonances.¹⁵⁻¹⁷ These two exciton states have the same hole component at all angles and differ only in the electron spin orientation (this can be recognized in Fig. 3; the electron Zeeman splitting is isotropic and, hence, the separation in energy of the two lowest-energy

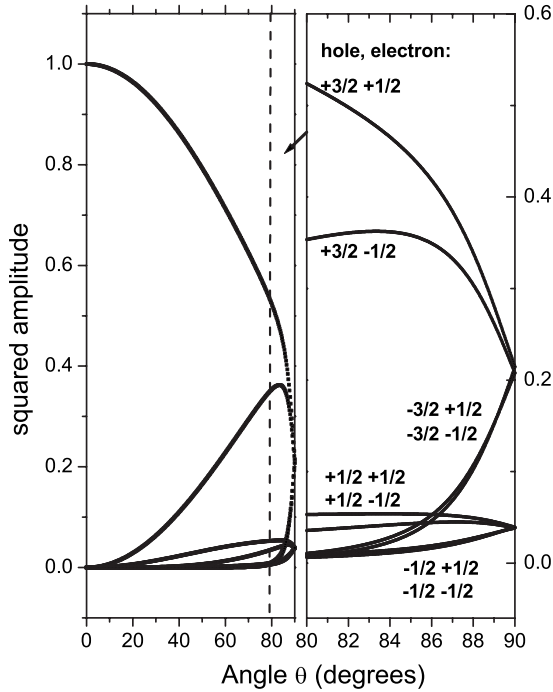


FIG. 4. Composition of the lowest-energy exciton wave function (relevant to the resonant excitation of PMR signals) as a function of the angle θ between the external magnetic field (6 T) and the growth axis. Left hand panel: the squared amplitudes of the basis functions $|m_j, m_s\rangle$ (quantized along the growth axis z); right hand panel: expanded view of the region close to the Voigt geometry, labeled by the $|m_j, m_s\rangle$ values.

states is independent of angle). The Raman scattering process therefore involves a spin-flip only of the electron component of the exciton, consistent with the experimentally observed selection rules which are that, in the Voigt geometry, the overtones are observed in the $z(\sigma\pi)\bar{z}$ polarization configuration (in conventional notation). Note that it is not a requirement of this process that the electron spin splitting should be identical to the change in energy of the Mn^{2+} system (experimentally, they are clearly not equal); a mismatch between these energies is possible because of the finite widths of the resonant intermediate X states.^{15,17}

In Fig. 5, we show a series of spin-flip Raman spectra for θ varying from 0° (Faraday) to 90° (Voigt) with a magnetic field of 6 T, with the excitation energies used being shown in Fig. 3. There is a clear decrease in n_{\max} with θ . This is expected on the basis of the existing model for the PMR overtones, which we now briefly summarize. The intensity $P_n(\tau)$ of the n th peak can be calculated using a Poisson distribution,^{1,6,18}

$$P_n(\tau) = \frac{1}{\tau} \int_0^\infty dt e^{-t/\tau} \frac{N(t)^n}{n!} e^{-N(t)}, \quad (2)$$

where τ is the lifetime of the exciton and $N(t)$ is the average change in the total spin of the Mn^{2+} ions interacting with the exciton of volume V . Note that, in Eq. (2), we omit a term representing the polarization selection rules; this term leads

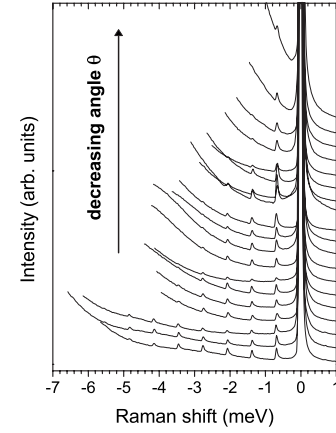


FIG. 5. Spin-flip Raman spectra as a function of the angle θ between the external magnetic field direction (6 T) and the growth axis from a 45 \AA single wide $\text{Cd}_{1-x}\text{Mn}_x\text{Te}/\text{Cd}_{1-x-y}\text{Mn}_y\text{Mg}_y\text{Te}$ quantum well ($x=0.0116$ and $y=0.12$). The angle θ ranges from 0° (top trace) to 90° (bottom trace) in steps of 5° .

to the prediction that odd- and even-numbered overtones should be observed only in crossed and parallel light polarizations, respectively,^{1,18} but its effects are generally not observed at low temperatures (here, $\sim 1.5 \text{ K}$) and for magnetic fields tilted by more than a few degrees with respect to the growth axis.¹⁸

In the above, $N(t)$ is given by

$$N(t) = \int_V dV n'_{\text{Mn}} S \sin \delta [1 - \cos(\omega_L t)]. \quad (3)$$

Here, n'_{Mn} is the density of Mn^{2+} ions, S is the total angular momentum of the ground state of Mn^{2+} , and the angle δ is between \mathbf{B}_{eff} and \mathbf{B}_{ext} . In terms of these fields, the precession frequency of the manganese ions ω_L is given by

$$\omega_L = \frac{g_{\text{Mn}} \mu_B}{\hbar} \sqrt{(B_{\text{ext}}^2 + B_{\text{exch}}^2 + 2B_{\text{ext}} B_{\text{exch}} \cos \theta)}. \quad (4)$$

When the external field is not orthogonal to the quantum well axis (which defines the direction of the exchange field), the term $B_{\text{ext}} B_{\text{exch}} \cos \theta$ in Eq. (4) is nonzero and it appears that the question of the sign of the exchange field with respect to the external field would arise. However, since $B_{\text{ext}} > B_{\text{exch}}$ (see below), the precession frequencies given by Eq. (4) for the two possible orientations of the exchange field only differ by about 30%.

In fact, once precession of the hole spin becomes possible (because of the development of a finite in-plane hole g factor g_\perp), an equally important question concerns the rate of the hole spin reorientation with respect to the other relevant time scales. Similar questions arise in the interpretation of quantum beats (QBs) in excitonic luminescence where, if the hole reorientation is fast, its exchange field is effectively zero and the quantum beats arise at the Larmor frequency of the electron in the exciton alone.¹⁹ On the other hand, if the hole orientation is stable on the time scale of the recombination process, then the QB frequency gains a contribution from the electron-hole exchange energy and is characteristic of the

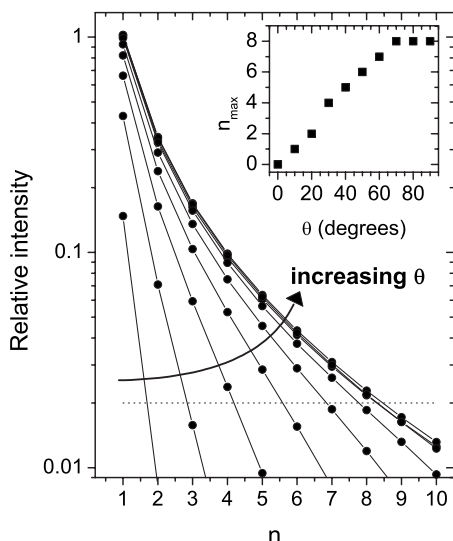


FIG. 6. Intensity (simulated) of n simultaneous spin flips ($\mathbf{B}_{\text{ext}}=6$ T) relative to the $n=1$ signal. The angle between \mathbf{B}_{ext} and \mathbf{B}_{exch} ranges in 10° steps from $\theta=10^\circ$ to $\theta=90^\circ$ [the relative intensity tends to zero for 0° (Faraday)]. The inset shows the number of peaks above the detection threshold intensity (the dashed line in the main figure) as a function of θ .

exciton.²⁰ The hole spin-flip rate has recently been shown to be crucial in the exciton spin decay process by a rather similar mechanism in nonmagnetic quantum well structures.²¹ These issues have been considered in Ref. 6 where, as noted earlier, it was shown that multiple overtones can still arise even in the presence of hole precession.

Using Eq. (2), therefore, we have calculated the relative intensities of the Raman peaks ($n=1, \dots, 10$) for a given angle θ , assuming $\mathbf{B}_{\text{ext}}=6$ T (Fig. 6). The following parameter values have been used based on those of Ref. 1 for similar quantum wells: $\tau=0.3$ ps, $(a_0)_{x,y}=30$ Å (exciton center of mass localization radius), and $\mathbf{B}_{\text{exch}}=+2$ T.⁶ When \mathbf{B}_{ext} is aligned along the quantum well growth axis ($\theta=0^\circ$), the probability $P_n(\tau) \rightarrow 0$, and hence this condition is omitted from the figure. We also note that Eq. (3) involves an integral over the exciton volume; we have investigated the consequences of changes in the exciton volume V as the angle θ is varied and find them to be small. For instance, a variation of the exciton wave function from a spherical shape to a shape with a cosinusoidal dependence on z gives a 20% variation in the number of Mn^{2+} ions within the exciton volume and a variation of less than 5% in the intensity of each overtone; the intensities of all overtones are reduced by similar factors, and our conclusions on the dependence of the number of

overtones on angle, described in the following, are not significantly affected. We have therefore taken the exciton volume to be independent of angle in the evaluation of $P_n(\tau)$.

In order to make a quantitative comparison of this calculation with the experimental data, we count the overtones experimentally observed and compare to the number predicted to lie above a cut-off intensity corresponding to our practical sensitivity limit (represented by the horizontal dashed line in Fig. 6, which, under the resonance conditions described earlier, corresponds to a cutoff after the $n=8$ signal at large values of θ). The number of PMR overtone signals above this line as a function of θ is shown in the inset of Fig. 6. The number of overtones above the sensitivity threshold steadily increases with θ , reaching a constant value ($n=8$) at 70° . This is in satisfactory agreement with the spin-flip Raman spectra in Fig. 5 and verifies the simple theory outlined in Sec. I. Strictly, this theory should hold only for values of θ in which J_z remains a good quantum number, i.e., for θ in the range from 0° to 80° (see Fig. 4), but good agreement with experiment is obtained even for values in the range of 80° – 90° , for which the more complicated theory of Ref. 6 might have been expected to be required.

IV. CONCLUSIONS

In summary, we have shown for a quantum well which contains magnetic ions that the number of multiple spin-flip Raman PMR signals monotonically decreases as the angle between the external magnetic field and the growth axis decreases. This observation, and even the actual number of overtones observed, is entirely consistent with the predictions of the simple theory in which precession of the magnetic moment of the manganese ions occurs about an effective magnetic field caused by combination of the external field with the exchange field that exists in the intermediate state. In order to understand the behavior, we have shown that proper account must be taken of the resonance enhancement of the scattering processes and, in particular, of the dependence of the resonance energies on the direction of the magnetic field.

ACKNOWLEDGMENTS

This work was supported by the EPSRC (U.K.), INTAS (03-51-5266), and the DFG (SFB 410). The work in Poland was partially supported by the Ministry of Science and Higher Education (Poland) through Grant No. N507 030 31/0735 and by the network “New materials and sensors for optoelectronics, information technology, energetic applications and medicine.”

¹J. Stühler, G. Schaack, M. Dahl, A. Waag, G. Landwehr, K. V. Kavokin, and I. A. Merkulov, Phys. Rev. Lett. **74**, 2567 (1995).

²J. Bao, A. V. Bragas, J. K. Furdyna, and R. Merlin, Nature (London) **2**, 175 (2003).

³M. Byszewski, D. Plantier, M. Sadowski, M. Potemski, A. Sa-

chrajda, Z. Wilamowski, and G. Karczewski, Physica E (Amsterdam) **22**, 652 (2004).

⁴S. A. Crooker, J. J. Baumberg, F. Flack, N. Samarth, and D. D. Awschalom, Phys. Rev. Lett. **77**, 2814 (1996).

⁵S. A. Crooker, D. D. Awschalom, J. J. Baumberg, F. Flack, and N.

- Samarth, Phys. Rev. B **56**, 7574 (1997).
- ⁶K. V. Kavokin and I. A. Merkulov, Phys. Rev. B **55**, R7371 (1997).
- ⁷J. J. Davies, D. Wolverson, O. Z. Karimov, and I. J. Griffin, J. Cryst. Growth **214/215**, 616 (2000).
- ⁸T. Wojtowicz, M. Kutrowski, G. Karczewski, and J. Kossut, Acta Phys. Pol. A **94**, 199 (1998).
- ⁹D. Suisky, W. Heimbrod, C. Santos, F. Neugebauer, M. Happ, B. Lunn, J. E. Nicholls, and D. E. Ashenford, Phys. Rev. B **58**, 3969 (1998).
- ¹⁰Q. X. Zhao, M. Oestreich, and N. Magnea, Appl. Phys. Lett. **69**, 3704 (1996).
- ¹¹R. Meyer, M. Dahl, G. Schaack, and A. Waag, Phys. Rev. B **55**, 16376 (1997).
- ¹²R. Romestain and C. Weisbuch, Phys. Rev. Lett. **45**, 2067 (1980).
- ¹³S. Maćkowski, E. Janik, F. Kyrychenko, and J. Kossut, Semicond. Sci. Technol. **14**, 979 (1999).
- ¹⁴B. Kuhn-Heinrich, W. Ossau, H. Heinke, F. Fischer, T. Litz, A. Waag, and G. Landwehr, Appl. Phys. Lett. **63**, 2932 (1993).
- ¹⁵J. Stühler, M. Hirsch, G. Schaack, and A. Waag, Phys. Rev. B **49**, 7345 (1994).
- ¹⁶M. Hirsch, R. Meyer, and A. Waag, Phys. Rev. B **48**, 5217 (1993).
- ¹⁷A. V. Koudinov, Y. G. Kusrayev, B. P. Zakharchenya, D. Wolverson, J. J. Davies, T. Wojtowicz, G. Karczewski, and J. Kossut, Phys. Rev. B **67**, 115304 (2003).
- ¹⁸J. Stühler, G. Schaack, M. Dahl, A. Waag, G. Landwehr, K. V. Kavokin, and I. A. Merkulov, J. Cryst. Growth **159**, 1001 (1996).
- ¹⁹A. P. Heberle, W. W. Rühle, and K. Ploog, Phys. Rev. Lett. **72**, 3887 (1994).
- ²⁰T. Amand, X. Marie, P. Le Jeune, M. Brousseau, D. Robart, J. Barrau, and R. Planel, Phys. Rev. Lett. **78**, 1355 (1997).
- ²¹G. V. Astakhov, A. V. Koudinov, K. V. Kavokin, I. S. Gaggis, Y. G. Kusrayev, W. Ossau, and L. W. Molenkamp, Phys. Rev. Lett. **99**, 016601 (2007).